

A volume-memory liquid

A. Han and Y. Qiao^{a)}

Department of Structural Engineering, University of California at San Diego, La Jolla, California 92093-0085, USA

(Received 22 August 2007; accepted 8 October 2007; published online 26 October 2007)

By dispersing nanoporous particles in an electrolyte solution, a “milklike” suspension is formed. At a low temperature, the nanoporous phase is hydrophilic, and thus the liquid can fill the nanopores spontaneously. As the temperature increases, the nanopore surfaces become hydrophobic. Consequently, the confined liquid defiltrates, leading to a significant system expansion. As the suspension works in between two different temperatures, it behaves as a thermal machine, exhibiting a volume-memory characteristic. Due to the large surface area, its energy density and the deformability are much higher than that of conventional shape-memory solids. © 2007 American Institute of Physics. [DOI: 10.1063/1.2803752]

For a few decades, shape-memory materials, also known as smart materials, have drawn increasing attention.¹ However, very often their energy density and deformability cannot meet the high functional requirements. One way to solve this problem is to use nanostructured materials to amplify beneficial surface energy exchange. For instance, by dispersing lyophobic nanoporous materials in liquid phases, advanced energy absorption systems can be developed.^{2–5} At ambient pressure, the liquid cannot enter the nanopores due to the capillary effect. As a quasihydrostatic pressure is applied, the liquid can infiltrate into the nominally energetically unfavorable nanopores. During this process, a significant amount of external work is converted to the excess solid-liquid interfacial tension $\Delta\gamma$. In some systems, the confined liquids do not defiltrate even when the external pressure is entirely removed, and thus the converted external work is dissipated. The specific absorbed energy can be calculated as $E^* = \Delta\gamma A$, where A is the specific surface area of the nanoporous material, typically ranging from 100 to 2000 m²/g. Because A is ultralarge, E^* can be two to three orders of magnitude higher than that of conventional damping or protective materials such as reinforced polymers.

In other nanoporous systems, especially when the nanopore size r is smaller than a few nanometer, the confined liquid can defiltrate out of the nanoporous space as the external pressure decreases. Such a system can be regarded as a “liquid spring.”⁶ Similar to the thermocapillary effect observed at large solid surfaces,⁷ the value of $\Delta\gamma$ in nanopores is temperature dependent.⁸ Thus, at various temperatures, the infiltration pressures are different. This phenomenon can be employed to develop “smart liquids”—nanoporous particle suspensions that can expand or shrink as temperature varies in a certain range. It has been discussed theoretically that such a mechanism does not violate thermodynamics laws.⁹ The energy density can be assessed as $E = \delta\gamma A$, with $\delta\gamma$ being the variation in $\Delta\gamma$ due to temperature change. As nanoporous materials of ultrahigh surface areas A are used, E can be as high as 10 J/g,¹⁰ larger than that of titanium-nickel (Ti–Ni) alloys by two orders of magnitude.

In the current study, we investigated a Zeolyst CBV-901 HY zeolite with the silica-to-alumina ratio of 80, the nominal

cation form of hydrogen, the Na₂O concentration of 0.03%, and the unit cell size of 24.2 Å. According to a gas absorption experiment, the specific surface area was 710 m²/g, the nanopore size was about 0.6 nm, and the specific nanopore volume was 0.22 cm³/g. The material was well crystallized,¹¹ with the particle size in the range of 10–50 μm. The zeolite was dehydrated in air at 150 °C for 3 h and exposed to silicon tetrachloride (SiCl₄) vapor in a nitrogen flow at 400 °C for 0.5 h. The treatment was performed in a vertical furnace with a cylindrical quartz reactor. The SiCl₄ treated zeolite was furnace cooled, washed repeatedly by distilled water until the pH value was close to 7, and calcined in air at 500 °C for 1 h. It was then dealuminated at 650 °C for 48 h in an air flow saturated with water steam, with the steam flow rate of 30 ml/min, followed by refluxing with a 7.5 wt % aqueous solution of ethylenediaminetetraacetic acid at 80 °C for 12 h. Finally, the particles were washed by warm water, filtered, and dried in vacuum.

The volume-memory experimental setup is depicted in Fig. 1. In a stainless steel cell, 1 g of zeolite was suspended in 7 g of 24 wt % aqueous solution of potassium chloride (KCl), forming a milklike liquid. The liquid was sealed by a steel piston. By using a type 5580 Instron machine, the piston was compressed into the steel cell at a constant rate of 0.5 mm/min. The pressure in the liquid phase and the system volume change were calculated as F/A_0 and $(d-d_0)A_0$, respectively, with F being the applied force, $A_0=286$ mm² the cross-sectional area of the piston, d the piston displacement, and d_0 the piston displacement of a reference system which contained the same amount of KCl solution but no zeolite.

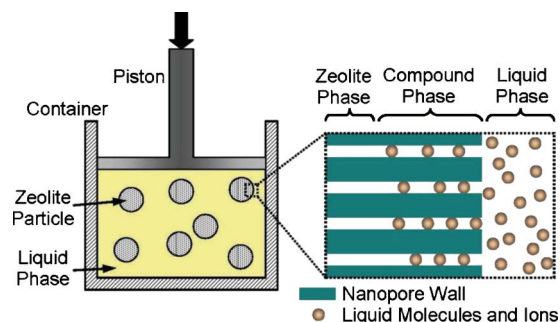


FIG. 1. (Color online) Schematic of the experimental setup.

^{a)}Electronic mail: yqiao@ucsd.edu

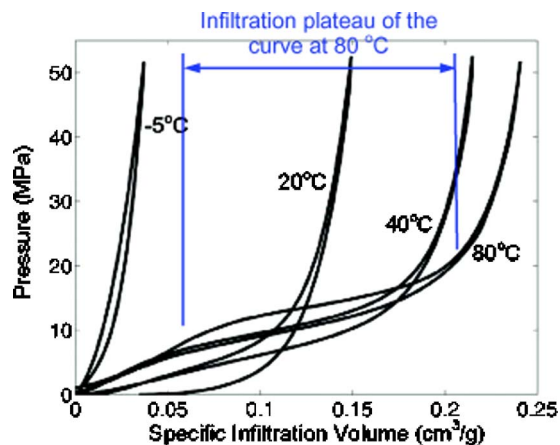


FIG. 2. (Color online) Typical sorption isotherm curves.

When the pressure exceeded 50 MPa, the piston was moved out of the steel cell at the same rate. Similar testing procedures were repeated at various temperatures in the range of -10 – 80 °C. Typical pressure-volume curves are shown in Fig. 2. The low temperatures were reached by using mixtures of liquid nitrogen and saturated sodium chloride solution, and the high temperatures were maintained by an Aldrich DigiTrol II Z28 water bath.

The addition of KCl in the liquid phase leads to the decrease in freezing point and the increase in wetting-nonwetting transition temperature. At room temperature, if no KCl were added, the zeolite is hydrophilic and the liquid infiltration can occur at zero pressure. If the liquid phase is a KCl solution, the nanopore walls become nonwetable. When the pressure reaches a critical value p_{in} , the liquid can be compressed into the nanopores, resulting in the formation of an infiltration plateau. Because the pore size is only 0.7 nm, across the cross section there are only a few water molecules or solvated ions, and thus the continuum theory, e.g., the Young's equation, is no longer valid. It is more appropriate to analyze the liquid infiltration process in the framework of pressure-induced phase transformation.

Initially, the zeolite phase and the liquid phase are separate. As liquid molecules enter nanopores, a compound phase is formed. When the entire zeolite phase transforms into the compound phase, the infiltration ends. As a first-order approximation, the equilibrium condition can be stated as $p\Delta V = \Delta\gamma A_{eff}$, where p is the external pressure, ΔV is the volume of liquid involved in the phase transformation, and $A_{eff} = \alpha 2\Delta V/r$ is the effective interface area, with α being the volume change ratio. At 80 °C, infiltration starts at about 10 MPa, where the capillary effect is overcome. If α is taken as 1, the above discussion would converge to the continuum theory, which leads to an estimation of $\Delta\gamma = 1.7$ mJ/m². The infiltration volume can be estimated by measuring the width of the infiltration plateau. As shown in Fig. 2, it is about 0.14 cm³/g, 40% smaller than the measured specific nanopore volume, indicating that $\alpha \approx 1.4$, which can be attributed to the promoted surface diffusion. Hence, the effective value of $\Delta\gamma$ should be 1.2 mJ/m². The compound phase is unstable as the pressure is lowered. At the defiltration pressure, p_d , the confined liquid molecules defiltrate out of the nanopores, causing the formation of a defiltration plateau. The difference between p_{in} and p_d may be related to the energy and mass exchanges between liquid and gas phases.¹² Note that the infiltration plateaus are not

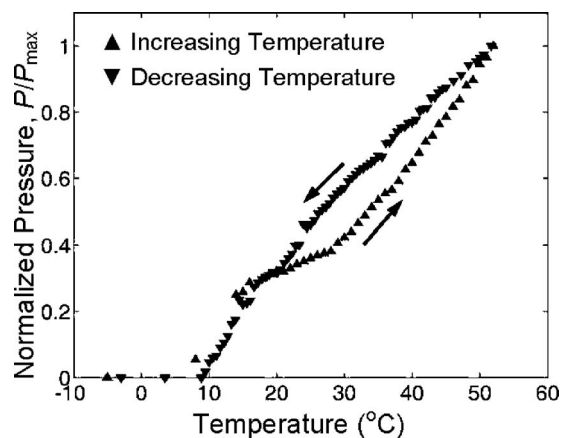


FIG. 3. The pressure as a function of the temperature when the system volume is kept constant.

flat, which may be related to the “internal friction” between the liquid molecules and the nanopore wall. In the relatively linear section of the infiltration plateau, the pressure increase is around 6 MPa. Using the most probable value of zeolite particle size, 40 μm , the pressure gradient along the axial direction in a nanopore can be assessed as 0.3 MPa/ μm , equivalent to an effective “adhesion” of 0.12 mJ/m² μm , smaller than 10% of $\Delta\gamma$, which looks plausible.

As shown in Fig. 2, when temperature rises, both p_{in} and p_d vary. At -5 °C, the nanopore surface is wettable to the liquid, and thus no infiltration can be observed during the loading-unloading process. Around 10–30 °C, wetting-nonwetting transition takes place. In this temperature range, while an infiltration plateau is formed, its width is considerably smaller. As temperature further rises, the infiltration plateau width reaches the saturated value. At a low temperature, when the liquid is confined in the nanopores, the total system volume is relatively small. If the system volume is kept constant and the temperature is increased, at a critical temperature T_{cr} , defiltration pressure becomes positive and the compound-to-zeolite phase transformation tends to occur. As a result, an internal pressure is generated. When the temperature is lowered, the pressure must be maintained to keep the system volume constant. Due to the difference between p_{in} and p_d , the decreasing temperature path tends to be higher than the increasing temperature path until the zeolite becomes effectively hydrophilic.

In the experiment, at -10 °C, 2 g of HY zeolite was immersed in 5.5 g of 24 wt % aqueous solution of potassium chloride and sealed in a steel cell (Fig. 1). Following a linear preloading cycle, the piston position was fixed by using a type 5580 Instron machine. The liquid pressure was initially kept at 0.05 MPa. The system was heated by an Aldrich DigiTrol II Z28 water bath. When the temperature reached 51 °C, the water bath was replaced by a mixture of liquid nitrogen and saturated sodium chloride solution. During the heating and cooling process, the liquid temperature was measured by a type-E thermocouple embedded in the steel cell. As shown in Fig. 3, at about 10 °C, the zeolite changes from hydrophilic to hydrophobic. The pressure rises continuously as temperature increases, and it decreases during cooling. The hysteresis, which is relatively small, is beneficial to maintain a stable pressure when temperature increases.

The thermally controlled expansion and shrinkage are more clearly shown in Fig. 4. The inset at the upper-left

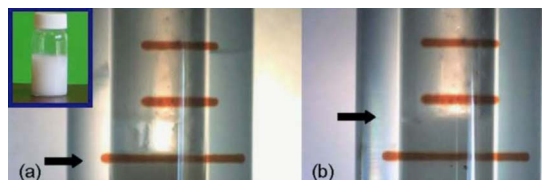


FIG. 4. (Color online) Photos of the volume-memory liquid (a) at $-5\text{ }^{\circ}\text{C}$ and (b) at $40\text{ }^{\circ}\text{C}$. The arrows indicate the liquid surfaces. The inset at the upper-left corner shows the milklike appearance.

corner shows the milklike appearance of the volume-memory liquid. At $-5\text{ }^{\circ}\text{C}$, 0.1 g of zeolite particles were suspended in 0.5 ml of 24 wt% aqueous solution of potassium chloride. Since the zeolite was effectively wettable, the system volume was relatively small. As temperature increased to $40\text{ }^{\circ}\text{C}$, the compound phase decomposed, and the system volume increased significantly by 0.012 ml, close to the total infiltration volume. As temperature was lowered to $-5\text{ }^{\circ}\text{C}$, the system volume was reduced back to the initial level. Thus, the system exhibits a volume-memory characteristic, compared with which the thermal expansion of a reference system that contains only 0.5 ml of potassium chloride solution is negligible.

For the experiment data, shown in Fig. 3, the maximum pressure reached at $51\text{ }^{\circ}\text{C}$, P_{max} , is 4.9 MPa. According to a Carnot cycle analysis,⁶ the net output energy is $\Delta\gamma A$ or $p_{\text{in}}V_{\text{in}}$, where V_{in} is the infiltration volume. If V_{in} is taken as $0.14\text{ cm}^3/\text{g}$, the specific energy density can be calculated as 0.7 J/g , much larger than that of Ti–Ni alloys (50 mJ/g). The deformability of the volume-memory liquid is dominated by the porosity of zeolite, which is about 20%, four to five times larger than that of Ti–Ni alloys. It is interesting that the internal pressure is quite linear to the temperature,

with the sensitivity of about $0.13\text{ MPa}/^{\circ}\text{C}$. The net output energy density is about $18\text{ mJ}/^{\circ}\text{C g}$.

To summarize, by functionalizing an electrolyte solution with a zeolite that has a thermally controllable surface wettability, a volume-memory liquid is developed. At a relatively low temperature, liquid molecules can enter the nanopores spontaneously, forming a compound phase. The compound phase decomposes as temperature rises, leading to an output energy density higher than that of conventional shape-memory alloys by orders of magnitude. Since the phase transformation is reversible, the liquid is of a volume-memory characteristic. It is envisioned that if the temperature field is nonuniform, the liquid can be shape memory.

The study was supported by The National Science Foundation and The Sandia National Laboratory under Grant No. CMS-0623973.

¹W. J. Buehler, J. V. Gilfrich, and K. C. Weiley, *J. Appl. Phys.* **34**, 1467 (1963).

²Y. Qiao, G. Cao, and X. Chen, *J. Am. Chem. Soc.* **129**, 2355 (2007).

³A. Han and Y. Qiao, *J. Am. Chem. Soc.* **128**, 10348 (2006).

⁴X. Chen, F. B. Surani, X. Kong, V. K. Punyamurtula, and Y. Qiao, *Appl. Phys. Lett.* **89**, 241918 (2006).

⁵F. B. Surani, A. Han, and Y. Qiao, *Appl. Phys. Lett.* **89**, 093108 (2006).

⁶M. Souillard, J. Patarin, V. Eroshenko, and R. Regis, *Stud. Surf. Sci. Catal.* **154**, 1830 (2004).

⁷P. C. Hiemenz and R. Rajagopalan, *Principles of Colloid and Surface Chemistry* (Dekker, New York, 1997).

⁸Y. Qiao, V. K. Punyamurtula, A. Han, X. Kong, and F. B. Surani, *Appl. Phys. Lett.* **89**, 251905 (2006).

⁹A. Laouir, L. Luo, D. Tondeur, T. Cachot, and P. Le Goff, *AIChE J.* **49**, 764 (2003).

¹⁰A. Han and Y. Qiao, *J. Mater. Res.* **22**, 644 (2007).

¹¹I. Halasz, S. Kim, and B. Marcus, *J. Phys. Chem. B* **105**, 10788 (2001).

¹²A. Han, X. Kong, and Y. Qiao, *J. Appl. Phys.* **100**, 014308 (2006).